

Interactions and effects of food additive dye Allura red on pepsin structure and protease activity; experimental and computational supports

Fatemeh Balaei¹, Mohabbat Ansari², Negin Farhadian³, Sajad Moradi^{2,*},
and Mohsen Shahlaei^{4,*}

¹Medical Biology Research Center, Health Technology Institute, Kermanshah University of Medical Sciences, Kermanshah, I.R. Iran.

²Nano Drug Delivery Research Center, Health Technology Institute, Kermanshah University of Medical Sciences, Kermanshah, I.R. Iran.

³Substance Abuse Prevention Research Center, Health Institute Kermanshah University of Medical Sciences, Kermanshah, I.R. Iran.

⁴Pharmaceutical Sciences Research Center, Health Institute, Kermanshah University of Medical Sciences, Kermanshah, I.R. Iran.

Abstract

Background and purpose: Today, color additives such as Allura red (AR) are widely used in different kinds of food products. Pepsin is a globular protein that is secreted as a digestive protease from the main cells in the stomach. Because of the important role of pepsin in protein digestion and because of its importance in digestive diseases the study of the interactions of pepsin with chemical food additives is important.

Experimental approach: In this study, the interactions between AR and pepsin were investigated by different computational and experimental approaches such as ultraviolet and fluorescence spectroscopy along with computational molecular modeling.

Findings/Results: The experimental results of fluorescence indicated that AR can strongly quench the fluorescence of pepsin through a static quenching. Thermodynamic analysis of the binding phenomena suggests that van der Waals forces and hydrogen bonding played a major role in the complex formation. The results of synchronous fluorescence spectra and Fourier transformed infra-red (FTIR) experiments showed that there are no significant structural changes in the protein conformation. Also, examined pepsin protease activity revealed that the activity of pepsin was increased upon ligand binding. In agreement with the experimental results, the computational results showed that hydrogen bonding and van der Waals interactions occurred between AR and binding sites.

Conclusion and implications: From the pharmaceutical point of view, this interaction can help us to get a deeper understanding of the effect of this synthetic dye on food digestion.

Keywords: Allura red; Enzyme activity; Molecular dynamics simulation; Pepsin; Spectroscopy study.

INTRODUCTION

Discovered evidence revealed that the ancient Egyptian were using color additives to make beverages and wines. Since various natural additives have been used to make foods more appetizing, artificial food colors are also nowadays widely used in many drinks and foods (1). Synthetic dyes are widely used

because of a wide range of benefits compared to natural colors, such as product simplicity, low cost of production, high solubility, better dyeing capacity, and unlimited use of dosage level (2).

Access this article online



Website: <http://rps.mui.ac.ir>

DOI: 10.4103/1735-5362.305189

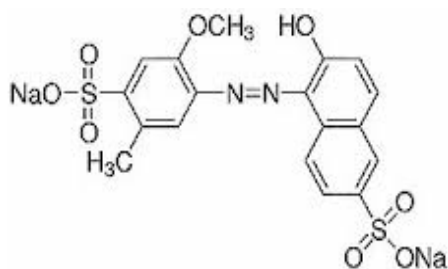
*Corresponding authors:

M. Shahlaei, Tel: +98-8334276489, Fax: +98-8334276493

Email: mshahlaei@kums.ac.ir

S. Moradi, Tel: +98-8334276489, Fax: +98-8334276493

Email: sajad.moradi@kums.ac.ir



Scheme 1. The molecular structure of Allura red synthetic dye.

Today, color additives are widely used to dye different kinds of drinks, foods, and sweets all over the world. Only 9 of these colors are FDA approved for use in the food industry that one of them is Allura red (AR) (3). AR (Scheme 1) has special chemical and physical properties, such as high solubility in water and high stability during industrial food processing. Based on a study published by Shimada *et al.* in 2010, AR can damage the DNA molecule in a rat's colon cells. Therefore, taking into account the potential dangers of AR for the human's body, consumption of this color by children is not recommended in Europe. Therefore, a more precise and controlled safety evaluation of this dye is of importance and the addition of AR to edibles industries must be controlled by regulatory bodies (4).

Pepsin is a globular protein which is secreted as a digestive protease from the main cells in the stomach and makes the smaller peptides by disrupting food proteins. The main action of pepsin is a breakdown of amide bonds next to the hydrophobic residues, especially those of tryptophan, tyrosine, and phenylalanine. Pepsin is a 35 kDa protein and has 326 amino acids (5) which structurally consists of two homologue domains; the N-terminal domain (amino acids 1-172) and the C-terminal one (amino acids 173-326). This protein mostly consists of the β -sheets and its catalytic site is lying among their main domains.

The catalytic site contains Asp32, Asp215 residues and for the enzyme to be active, one of them remaining protonated and the other is deprotonated (6). Investigating the interactions between exogenous ligands and biomacromolecules such as DNA and proteins is very important, hence these interactions can interfere with the homeostasis in the function of

macromolecules (7). In this regard, in addition to experimental spectroscopic techniques (8), the computational molecular modeling approaches are also employed (9,10). Recently, some studies on the interaction between different ligands and pepsin have been reported. Ying *et al.* studied the pepsin-curcumin interactions using experimental methods and molecular docking (5).

The results showed that upon binding curcumin to pepsin, its intrinsic fluorescence can significantly be quenched. Also, the docking results indicated that the residues of Thr77, Thr218, and Glu287 were involved in the interaction through hydrogen bonding. In other studies, Wu *et al.* have investigated the interaction between AR and human serum albumin (11) and the static manner was reported as the mechanism of fluorescence quenching for the interaction. The hydrogen bond and van der Waals forces were found to have the main roles in the interaction between AR and human serum albumin as the thermodynamic parameters have negative values. Because of the important role of pepsin in the protein digestion and the fact that the abnormalities in its activity may cause gastrointestinal problems, the study of the interactions of pepsin with chemical food additives is important. Therefore, in this study, the interactions between AR and pepsin were investigated by experimental methods along with molecular modeling studies.

MATERIALS AND METHODS

Chemicals

Pepsin from the porcine gastric mucosa was prepared from MERCK (Germany). AR, Folin reagent, and casein were purchased from Sigma-Aldrich (USA). The activity measurements were done in sodium citrate-citric acid buffer, pH 2.5.

Absorption measurements

The absorption spectrums were recorded in the absence and presence of AR (incremental concentrations of 0.3, 0.6, 0.9, 1.2, 1.5, 1.8 μ M) in the wavelength range of 245-350 nm using a UV-visible optical spectrophotometer (Agilent 8453, Germany-USA) applied a 1.0 cm cuvette.

Fluorescence measurements

In this study, the fluorescence spectrums were collected in a Perkin Elmer fluorescence spectrofluorimeter (LS55) using the excitation wavelength of 285 nm and the emissions from 300-500 nm at 293, 398, and 303 K, respectively. The pepsin solution (1 μ M) was titrated with an AR concentration range of 1-6 μ M

The correction of the inner-filter effect was done using the Beer-Lambert equation:

$$F_{corr} = F_{obs} \text{antilog}[(A_1 + A_2)/2] \quad (1)$$

where, F_{corr} and F_{obs} are respectively the corrected and measured fluorescence intensities. A_1 and A_2 are the excitation and emission wavelengths of the ligand respectively (5).

The synchronous fluorescence of $\Delta\lambda = 15$ and $\Delta\lambda = 60$ nm was obtained from 250 nm to 350 nm, at excitations of 280 and 295, respectively (12).

Measuring enzyme activity

The enzyme activity measurements were done using Anson's method along with some modifications (13). Briefly, 300 μ L of pepsin solution (500 μ M) in citric acid-sodium citrate buffer were incubated with an equal volume of casein (100 μ L of 3% w/v at 38 °C for 20 min; final volume was 1500 μ L). The reaction was then disrupted by adding 1 mL of 3% w/v trichloroacetic acid and the final solution was centrifuged for 10 min at 12000 rpm at -4 °C. Then, the 0.5 mL of the supernatant solution was added to 1 ml of 0.2 M Na_2CO_3 solution. In the next step, 0.1 mL of the Folin ciocalto's solution diluted in water (ratio 2:1) was added and the resulted solution was alkalized using 0.2 mL NaOH (10 M). Finally, the solution was maintained at 37 °C for 10 min. The absorbance was then recorded at 625 nm. The activity of enzymes in proteolytic activity units per mL (PAU/ml) was calculated using the following equation (14):

$$\text{PAU/mL} = \frac{A \times V}{A_1 \times t} \quad (2)$$

where A is the absorbance of a sample, A_1 is the absorbance of 1 mEq of tyrosine (1620), V is the sample volume and t is the reaction time, respectively.

Furrier transform infra-red spectroscopy

Furrier transform infra-red (FTIR) spectra of free pepsin and pepsin-AR (subtracted by AR spectrum) were recorded in a Shimadzu IR2000 spectrophotometer (Japan). The IR spectra were taken over a range of 400-4000 cm^{-1} by the resolution of 8 cm^{-1} and 100 scans.

Molecular modeling

To investigate the location and the mode of interaction between AR and pepsin in atomistic details, the molecular modeling methods were used. In this regard, at first, a stable and low-energy complex was obtained using AutoDock4 software (15,16). The PDB code of 3UTL obtained taken from the RCSB protein data bank was as a 3D structure of the pepsin (17,18). After manually removing the crystallographic water molecules, the addition of Gasteiger-Marsili charges was done using the AutoDock Tools software (19). Also, the structure of AR was sketched using the ACD/LAB software and its 3D conformation was developed in Avogadro software (20). Atomic charges were calculated by the Gasteiger method and all rotational bonds were considered active. Eventually, atomic types related to the AutoDock force field were determined for all atoms. Energetic maps for the atomic types of the ligand were calculated in the search space in such a way that they can explore all portions of the protein that were obtained using the AutoGrid 4 software. Finally, the molecular docking was done in the AutoDock 4 by 250 runs under the Lamarckian genetic algorithm (21).

The lowest energy of ligand conformation in the cluster with the highest number in considering the root-mean-squared deviation (RMSD) less than 0.2 nm and binding energy greater than -6 kcal/mole was selected for further study. The dynamics of the protein-ligand complex were investigated using the molecular dynamics simulation technique. To this end, the topological information of the ligand was obtained using the ATB server (22) and the simulations were done using Gromacs 5.1 package in the Gromos53a6 force field (22,23). The box was then solvated by SPC/E water molecules and in order to completely neutralize the system, enough counter ions were

added (24). The system energy was minimized using the steepest descent algorithm (25). Applying the NVT and NPT ensembles respectively, the equilibration of temperature and the pressure was performed to 298 K and 1 bar. To this end, the V-rescale thermostat (26) along with the Parrinello-Rahman barostat were used, respectively (27). All bonds were constrained using the LINCS method (13). The van der Waals interactions using Lennard Jones methods and electrostatic ones with a Particle Mesh Ewald (PME) both were calculated up to a radius of 1 nm (28). Finally, the free pepsin and pepsin-ligand systems were simulated for 50 ns under a leapfrog approach of molecular dynamics. Graphical representations were prepared using visual molecular dynamic (VMD) software (29,30) and LigPlot (www.ebi.ac.uk/thornton-srv/software/LigPlus).

RESULTS

Spectroscopy studies

UV-vis absorption spectra

UV-vis absorption spectra of protein were recorded in the absence and presence of increasing concentrations of AR and shown in (Fig. 1).

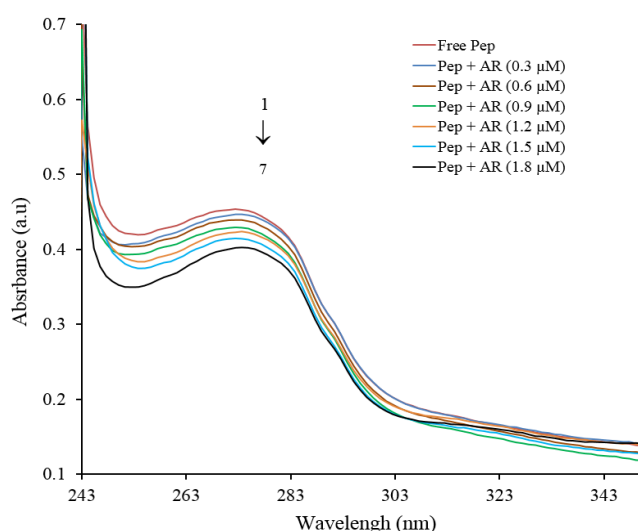


Fig. 1. Absorption spectra of pepsin and pepsin + AR complexes at different concentrations. AR, Allura red.

The results indicated that by increasing the dye concentration the absorption intensity of protein is decreased significantly. Also, as it can be seen from the figure there is no right or left shift in the peak position of UV-vis spectra.

Fluorescence quenching spectra studies

The effect of incremental concentrations of AR on the pepsin intrinsic fluorescence spectra is shown in (Fig. 2). As can be seen, in the presence of incremental concentrations of AR a decrease in the fluorescence intensity of pepsin is observed.

To determine the type of quenching mechanism of pepsin by AR, the fluorescence investigations were performed at several temperatures (293, 298, and 303 K) and decrement in emission intensities were analyzed. The final results are shown in Fig. 3A and reported in Table 1.

Analyzing of thermodynamic parameters

The binding sites and the binding constants of AR to the protein can be determined using the intercept and the slope of the modified Stern-Volmer curve at various temperatures. The final results of the modified Stern-Volmer analysis are shown in Fig. 3B and details are reported in Table 2 (31).

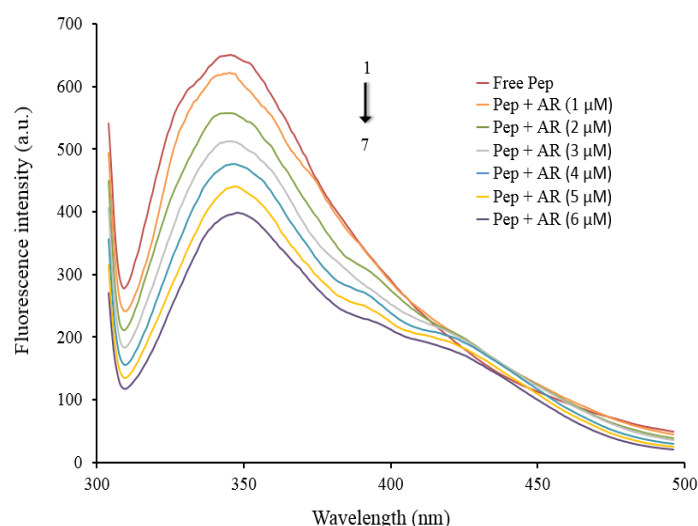


Fig. 2. The intrinsic fluorescence spectra of pepsin in the absence and presence of AR at 1-6 μM . AR, Allura red.

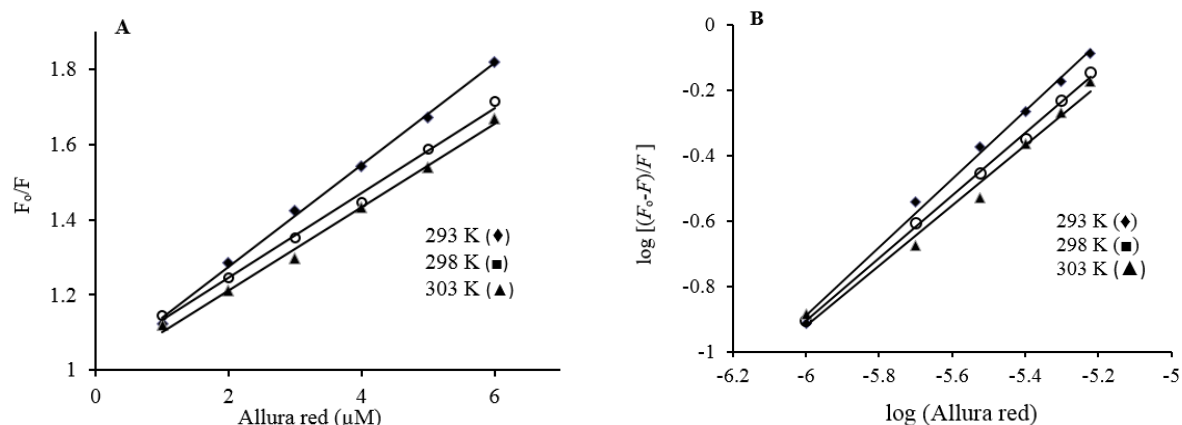


Fig. 3. (A) The Stern-Volmer plots and (B) the modified Stern-Volmer plots for fluorescence quenching of pepsin by Allura red at 293, 298, and 303 K.

Table 1. The Stern-Volmer quenching constant (K_{SV}) and quenching rate constant (k_q) for binding of Allura red to pepsin at different temperatures.

| Complex | Temperature (K) | $K_{SV} \times 10^5 (M^{-1})$ | $k_q \times 10^{13} (M^{-1} s^{-1})$ | R^{2*} |
|-------------------|-----------------|-------------------------------|--------------------------------------|----------|
| Allura red-pepsin | 293 | 1.36 ± 0.11 | 1.36 ± 0.11 | 0.99 |
| | 298 | 1.13 ± 0.17 | 1.13 ± 0.17 | 0.96 |
| | 303 | 1.11 ± 0.13 | 1.11 ± 0.13 | 0.98 |

* R^2 Is the correlation coefficient for the K_{SV} values.

Table 2. The binding constant (K_b) and the number of binding sites (n) for binding of Allura red to pepsin at studied temperatures.

| Complex | Temperatures(K) | $K_b \times 10^3 (M^{-1})$ | n | R^2 |
|-------------------|-----------------|----------------------------|------|-------|
| Allura red-pepsin | 293 | 234.21 ± 4.06 | 1.04 | 0.96 |
| | 298 | 71.60 ± 1.68 | 0.96 | 0.98 |
| | 303 | 40.59 ± 2.45 | 0.92 | 0.98 |

Data are expressed as mean \pm SD of three measurements.

Table 3. Thermodynamic parameters for binding of Allura red to pepsin.

| Complex | Temperatures (K) | $\Delta S^\circ (J mol^{-1}K^{-1})$ | $\Delta H^\circ (kJ mol^{-1})$ | $\Delta G^\circ (kJ mol^{-1})$ |
|-------------------|------------------|-------------------------------------|--------------------------------|--------------------------------|
| Allura red-pepsin | 293 | | | -0.039526 ± 0.93 |
| | 298 | -352.42 ± 4.92 | -133.30 | -28.277436 ± 1.18 |
| | 303 | | | -26.515346 ± 2.08 |

Data are expressed as mean \pm SD of three measurements.

In order to characterize the major forces involve in the formation of a complex between AR and pepsin, thermodynamic parameters including the enthalpy change (ΔH), the entropy change (ΔS), and the changes in Gibbs free energy (ΔG) were calculated. These parameters by using related relations were calculated and listed in Table 3.

FTIR spectroscopy

The FTIR spectra of pepsin in the absence and presence of AR are illustrated in Fig. 4. As can be seen, the intensity of beta amide bands

in both regions ($1622-1627$ and $1628-1637 cm^{-1}$) and ($1697-1703 cm^{-1}$) was increased after complex formation. These results also show that there is no significant right or left shifts in the peak situation implying that there is no destructive effect of AR on the protein structure.

Synchronous spectroscopy

The results for synchronous fluorescence spectra of protein in the absence and presence of various concentrations of AR at the wavelength interval ($\Delta\lambda$) of 15 and 62 nm are shown in Fig. 5A and B, respectively.

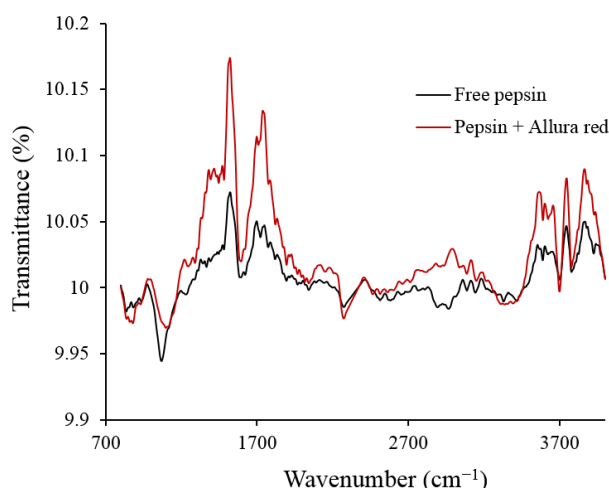


Fig. 4. FT-IR spectra of pepsin and Allura red pepsin complex (concentration ratio 1:1)

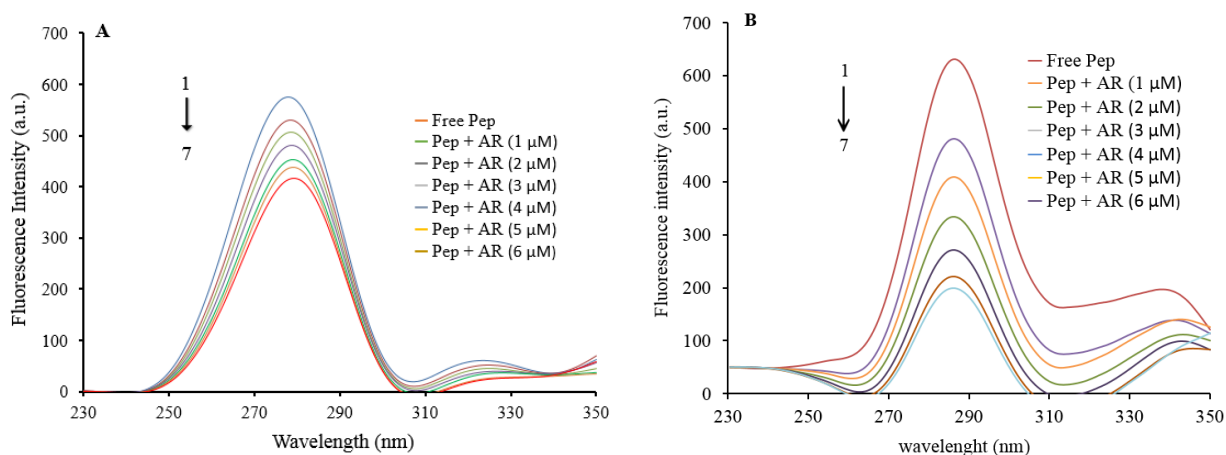


Fig. 5. Synchronous fluorescence spectrum (A) $\Delta\lambda = 60$ nm and (B) $\Delta\lambda = 15$ nm of pepsin ($0.4 \mu\text{M}$) in the absence and presence of Allura red.

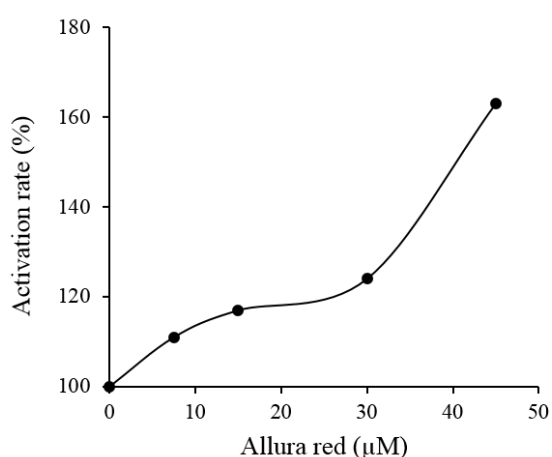


Fig. 6. Effect of Allura red on pepsin activity *in vitro* at 310 K.

Investigate pepsin protease activity

The enzyme activity was measured using equation 2 and the obtained results are shown in Fig. 6. As shown in this figure, with increasing

concentrations of AR, the enzyme activity increased. In addition, the activation rate is %163 when the concentration of AR is $45 \mu\text{M}$.

Molecular modeling

Docking

The molecular docking results are shown in Fig. 7. As shown in this figure, most of the forces involved in the interaction are of the type of hydrogen bonding and van der Waals forces (Fig. 7A). Similarly, the results of the docking analysis predict the main interaction site is close to the active site of pepsin (Fig. 7B).

Molecular dynamic simulation

In the first step, in order to ensure that the systems reached the equilibrium and to investigate the severe structural change in the protein, both in free and ligand bonding states,

its *RMSD* was studied and the results are shown in Fig. 8. The root-mean-squared fluctuation (*RMSF*) analysis also indicates a general and local decrease in protein amino acid fluctuations in the presence of ligand (Fig. 9).

Using the definition secondary structure of protein (*DSSP*) analysis, structural changes of

protein was also examined in terms of the number of residues in the secondary structures and structural displacements, and Fig. 10 shows the results of this study.

The radius of gyration (*R_g*) which is an index of compression or swelling of protein was measured and its results are shown in Fig. 11.

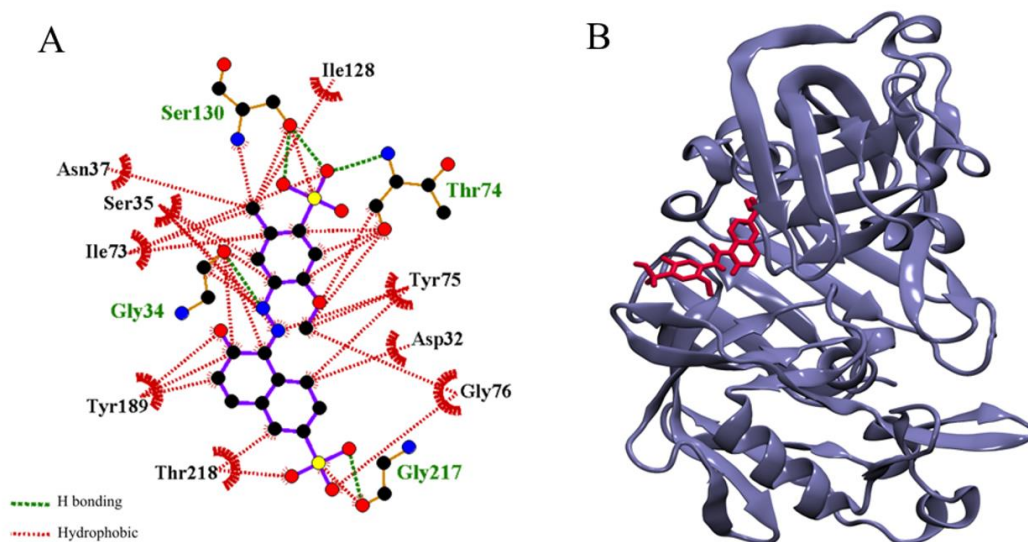


Fig. 7. Results of docking analysis of Allura red on pepsin, (A) 2D and (B) 3D illustrations of the ligand-protein interaction.

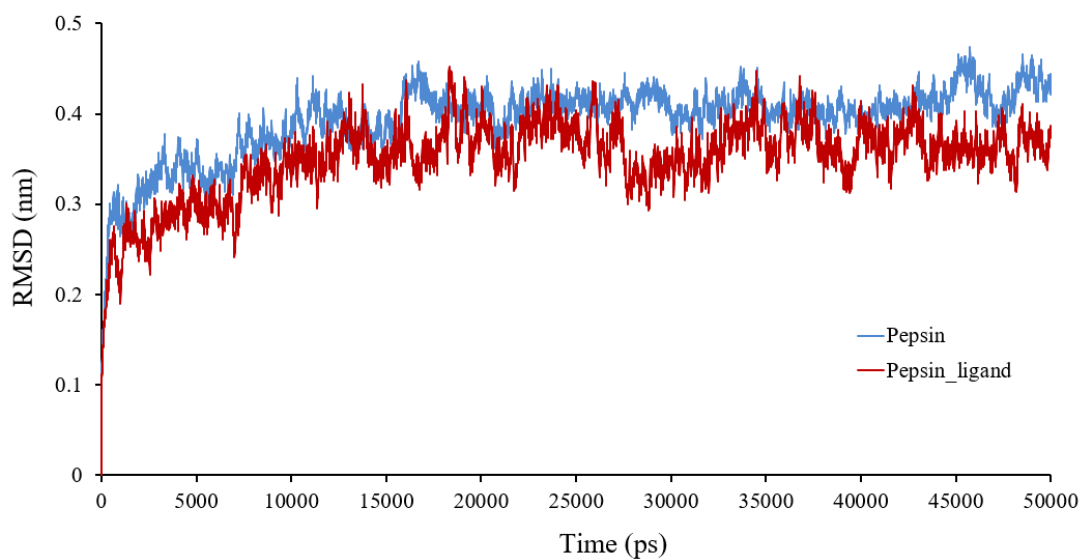


Fig. 8. Root mean squared deviation of carbon alpha during the molecular dynamic simulation.

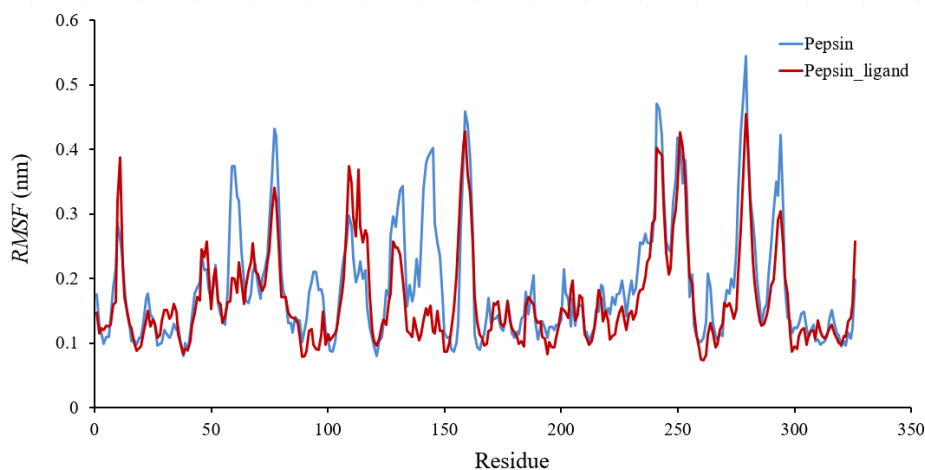


Fig. 9. Root mean squared fluctuation of amino acids with respect to their mean mobility.

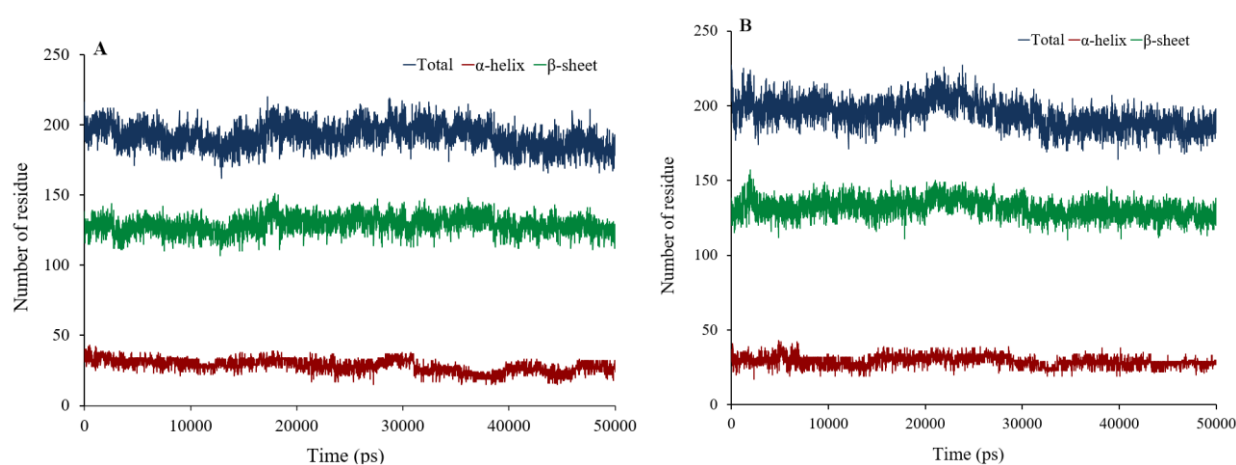


Fig. 10. Secondary structure analysis obtained by DSSP method for (A) free pepsin and (B) pepsin-Allura red.

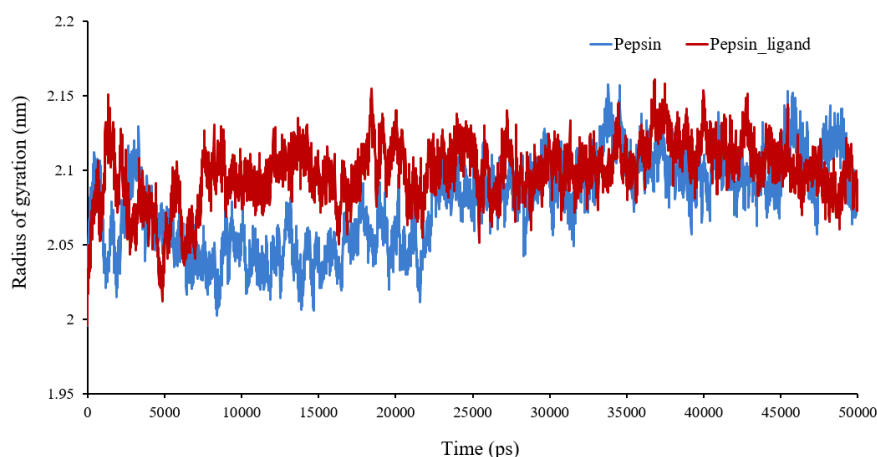


Fig. 11. Changes in the radius of gyration for free protein and protein in complex with Allura red.

DISCUSSION

The UV-vis absorption spectra of pepsin decreased in the presence of an increasing concentration of AR (Fig. 1). A reduction in the maximum absorption spectrum of the protein at the presence of the ligand was

observed that can be a sign for the formation of a complex between in the amount of AR (32). There were no significant changes in the peak location that can be an indication of lacking significant conformational changes in the protein structure (13,33).

Generally, the aromatic amino acid residues of proteins (including tryptophan, tyrosine, and phenylalanine) have indole moieties that they are very sensitive to polarity changes in the environment, therefore a suitable method to peruse the structural changes of the protein upon ligand binding is the fluorescence spectroscopy (34). As can be seen (Fig. 2) in the presence of incremental concentrations of AR a decrease in the fluorescence intensity of pepsin is observed that refers to the presence of aromatic residues, especially tryptophan and tyrosine residues close to the AR binding site (35).

Fluorescence quenching occurs through two mechanisms: dynamic and static quenching. These different mechanisms can be distinguished through their different dependency on the variation in viscosity and temperature (36). In the dynamic quenching, with increasing temperature due to the higher diffusion rate, the collision between the quencher and fluorophore is increased results in more fluorescence quenching. In comparison, in a static quenching mechanism, with increasing temperature, the stability of the fluorophore and the quencher complex decreases, and thus, the result of increasing temperature is reducing the quenching constant (34).

So, to characterize the quenching mechanism of pepsin in the presence of AR, the fluorescence investigations were done at several temperatures and decrement in emission intensities was analyzed from the Stern-Volmer relation (equation 3):

$$F_0/F = 1 + K_q\tau_0[Q] = 1 + K_{sv}[Q] \quad (3)$$

where the value of F_0 and F explain the fluorescence emission intensities of protein in the absence and presence of the AR, respectively, K_q is the quenching constant, K_{sv} is the Stern-Volmer constant, $[Q]$ is the molar concentration of the quencher and τ_0 is the fluorophore lifetime in the absence of quencher which its value for proteins is 10^{-8} s (37).

The values of K_{sv} were calculated from the slope of the Stern-Volmer plots. The pepsin concentration was in 0.2 mM sodium citrate buffer, pH 2.5. Standard deviations were approximately within 5% of the experimental

values of three independent experiments. For more details, please see Fig. 3 and Table 2.

As can be seen, the Stern-Volmer plots of pepsin and AR complex were linear and there is an inverse relationship between the slopes and the temperature.

The results obtained from the analysis of the Stern-Volmer plots showed that the quenching mechanism of the pepsin by AR is static, therefore, the formation of a complex between pepsin and ligand decreases with the rising temperature. According to the literature, in the case where the K_q is more than the value of 10^{10} , the quenching is static; otherwise, it is of a dynamic type (38). The results reported in Table 1 show that the K_b values for AR-pepsin complex in any temperature are more than the mentioned cut off, it can be concluded that a stable complex between protein and ligand make the quenching mechanism static.

The binding of small molecules to a biomacromolecule with equivalent sites can be analyzed from the modified Stern-Volmer relation according to the following equation:

$$\log \{(F_0 - F)/F\} = \log K_b + n \log [Q] \quad (4)$$

where K_b is the binding constant of the ligand to the biopolymer and n is the number of binding sites per biopolymer (38). According to the analysis of the modified Stern-Volmer that listed in Table 2 the value of binding constant K_b decreases with increasing temperature and it shows that the protein-quencher complex is more unstable at the higher temperatures. These results confirmed that the mechanism played a major role in the quenching of pepsin is the static quenching mechanism.

In the non-covalent interaction of ligands and biomolecules, four major forces are involved, hydrogen-bonding interaction, van der Waals' forces, electrostatic interactions, and hydrophobic forces (31). The enthalpy and entropy changes were obtained from the Van't Hoff equation as follows:

$$\ln K_b = -(\Delta H_0/RT) + (\Delta S_0/R) \quad (5)$$

where T is the temperature of the experiment, R is the gas universal constant (8.314 J/K.mol) and K_b is the apparent binding constant at the corresponding temperature which was calculated using equation 4 (39). The values of enthalpy and entropy changes obtained from the

slope and intercept of linear Van't Hoff diagram by plotting $\ln K_b$ against $1/T$. Afterward, using the thermodynamic equation (equation 6), the Gibbs energy was calculated at different temperatures. The thermodynamic parameters were then calculated and listed in Table 3.

$$\Delta G_0 = \Delta H_0 - T\Delta S_0 \quad (6)$$

The negative values of Gibbs energy suggested that the formation of the complex between pepsin and AR is a spontaneous process (40,41). According to Ross and Olsson's theory, when enthalpy and entropy changes are negative, the major force in ligand binding are hydrogen bond and van der Waals force, when these two values are positive, the main force in the ligand-binding is hydrophilic interactions and when the values of enthalpy change and entropy change are negative and positive respectively, electrostatic forces play an important role in stabilizing the interaction (12). Therefore, as Table 3 shows, the main forces that have a major role in the formation of the complex between pepsin and AR are the hydrogen bond and the van der Waals forces.

In this study, the protease activity of enzyme was investigated in the absence and presence of increasing concentrations of AR in 0.2 mM sodium citrate buffer and pH 2.5. The results clearly showed that in the presence of AR, enzymatic activity of pepsin was increased. From a medical point of view, the increasing protease activity of pepsin may lead to digestive problems such as duodenal ulcer disease, gastric ulcer, and also gastrointestinal bleeding.

FTIR spectroscopy is a useful method for probing changes in the secondary conformation of proteins upon ligand binding. The IR data recorded from proteins illustrate the existing three main amide band I (1600-1700 cm^{-1}), amide band II (1500-1550 cm^{-1}) and amide band III (1855-2873 cm^{-1}) in their spectra which are highly sensitive to protein conformational changes (42). Among the various amide bands, amide band I is more remarkable because it is sensitive than others to conformational changes of the proteins and thus is widely used to demonstrating changes in the secondary structure of proteins due to ligand binding (43). The peak position of amide I

occurs in 1600-1700 cm^{-1} region (due to the C=O stretching mode) that is especially sensitive to β -sheet structures, whereas the amide II band emerges in 1500-1600 cm^{-1} (due to N-H bending that coupled with C-N stretching modes) (41). The obtained results from this analysis show that there is no significant right or left shift in peak position which indicating that the secondary structure of protein did not changed in complex with AR.

Generally, the spectra obtained from the synchronous fluorescence studies can give useful information about conformational changes of protein during the ligand binding and also the molecular environment of a fluorophore. The synchronous spectra provide specific information about the tryptophan residues at the maximum wavelength interval, between excitation and emission wavelength, ($\Delta\lambda$) of 60 nm, while the spectra corresponding to $\Delta\lambda$ of 15 nm provides information about the tyrosine residues (12). The fluorescence intensity of pepsin was decreased gradually with an increase in the concentration of AR and the decrease in $\Delta\lambda$ of 15 nm was more than those of 60 nm. The obtained binding constant values using Stern-Volmer equation at the wavelength interval ($\Delta\lambda$) of 15 and 60 nm were calculated and the results showed that the values were 52.88×10^4 and $61.48 \times 10^3 \text{ M}^{-1}$, respectively. These results indicate that the AR binds to a position close to the tyrosine residues.

The molecular docking results in agreement with the experimental data showed strong interactions and formation of the AR-pepsin complex. As can be seen in Fig. 7 and in agreement with the experimental results, there are a few numbers of hydrogen bonding between the protein and ligand that, in conjunction with the van der Waals interactions, make it possible to form a stable binding between the ligand and protein.

In view of these results, it can be concluded that the most important amino acids in the interaction are threonine 74 and glycine 76. Also, due to the close ligand binding of tyrosine residues 75 and 189, a further reduction in the fluorescence of tyrosine residue than those of tryptophan may be associated with a greater contact of AR with tyrosine.

The docking result is related to the interactions between the rigid proteins with ligand and therefore, there is a need for molecular dynamic simulations to obtain complementary information on its binding to flexible protein and evaluation of dynamics of interactions. In this study, after preparing the stable ligand-protein complex with the lowest possible energy, their dynamic interaction was studied using molecular dynamics and the results were compared with those of free protein.

Based on the results reported from *RMSD* studies, both systems have reached a relatively stable equilibrium point after 15 ns, followed by small fluctuations to the end of the simulation. These results also indicated that the total amount of *RMSD* has decreased in the ligand-protein system that can be a sign for the more structural rigidity of protein after binding of the ligand. Also, as can be seen in the ligand-binding regions, the majority of amino acids exhibited less mobility, which can indicate more protein stability.

In order to investigate the effects of AR on the secondary structure of protein, the *DSSP* analysis was performed. Figure 10A shows that there is no significant difference between free protein and ligand-protein systems. On the other hand, structural stability in the ligand-protein system has increased slightly in comparison to the free protein (Fig. 10B). Regarding the obtained results, it seems that the binding of the ligand by inhibiting and reducing protein fluctuations has led to the stability of its secondary structures. These results, in addition to *RMSD* and *RMSF* analysis, are in agreement with the experimental results of UV and FTIR, and show the stability of the protein secondary structure during the interaction with ligand.

Based on the results of the *Rg* which were studied for evaluating of protein compression or swelling, it can be seen that the *Rg* values of both proteins are similar in the matter of value and its fluctuations in the equilibrated state. Briefly, these results, in good agreement with experimental results, confirm the positive effects of the ligand on the structural stability of the protein, which can ultimately be one of the reasons for the enzyme's improved function and protein activity.

CONCLUSION

In the studies done in this article, the interaction of AR with pepsin has been investigated using various spectroscopic studies and molecular modeling techniques. The results from both studies indicated that a stable complex of AR and pepsin is occurred, and the van der Waals forces along with hydrogen bonds have the main rule in the complex formation. Also, the enzyme activity assay revealed that the formation of a complex between AR and pepsin result in the activity of pepsin was increased. The FTIR spectra showed that the complex formation between AR and pepsin leads to a slight increase in the beta-sheet and α -helix of the protein. All results of molecular modeling studies imply the formation of a stable complex between AR and pepsin that resulted in the structural stability of the protein and these results are in agreement with the experimental data. From the pharmaceutical point of view, this interaction can help us to get a deeper understanding of the effect of this synthetic dye on food digestion. Investigating the factors affecting the activity of pepsin in the stomach can be effective in the treatment of diseases influenced by pepsin activity including stomach ulcers and duodenal diseases.

Acknowledgments

This work was financially supported by the Vice-Chancellery of Research of Kermanshah University of Medical Sciences under Grant No. 97437.

Conflict of interest statement

The authors declared no conflict of interest in this study.

Authors' contribution

All authors contributed equally to this work.

REFERENCES

1. Oplatowska-Stachowiak M, Elliott CT. Food colors: existing and emerging food safety concerns. *Crit Rev Food Sci Nutr.* 2017;57(3):524-548. DOI: 10.1080/10408398.2014.889652.
2. Downham A, Collins P. Colouring our foods in the last and next millennium. *Int J Food Sci Technol.* 2000;35(1):5-22. DOI: 10.1046/j.1365-2621.2000.00373.x.

3. Stevens LJ, Burgess JR, Stochelski MA, Kuczek T. Amounts of artificial food dyes and added sugars in foods and sweets commonly consumed by children. *Clin Pediatr (Phila)*. 2015;54(4):309-321. DOI: 10.1177/0009922814530803.
4. Wang L, Zhang G, Wang Y. Binding properties of food colorant allura red with human serum albumin *in vitro*. *Mol Biol Rep*. 2014;41(5):3381-3391. DOI: 10.1007/s11033-014-3200-z.
5. Ying M, Huang F, Ye H, Xu H, Shen L, Huan T, *et al*. Study on interaction between curcumin and pepsin by spectroscopic and docking methods. *Int J Biol Macromol*. 2015;79:201-208. DOI: 10.1016/j.ijbiomac.2015.04.057.
6. Shen L, Xu H, Huang F, Li Y, Xiao H, Yang Z, *et al*. Investigation on interaction between Ligupurpuroside A and pepsin by spectroscopic and docking methods. *Spectrochim Acta A Mol Biomol Spectrosc*. 2015;135:256-263. DOI: 10.1016/j.saa.2014.06.087.
7. Bijari N, Balalaie S, Akbari V, Golmohammadi F, Moradi S, Adibi H, *et al*. Effective suppression of the modified PHF6 peptide/1N4R Tau amyloid aggregation by intact curcumin, not its degradation products: another evidence for the pigment as preventive/therapeutic “functional food”. *Int J Biol Macromol*. 2018;120(Pt A):1009-1022. DOI: 10.1016/j.ijbiomac.2018.08.175.
8. Jafari F, Moradi S, Nowroozi A, Sadrjavadi K, Hosseinzadeh L, Shahlaei M. Exploring the binding mechanism of paraquat to DNA by a combination of spectroscopic, cellular uptake, molecular docking and molecular dynamics simulation methods. *New J Chem*. 2017;41:14188-14198. DOI: 10.1039/C7NJ01645J.
9. Moradi S, Hosseini E, Abdoli M, Khani S, Shahlaei M. Comparative molecular dynamic simulation study on the use of chitosan for temperature stabilization of interferon α I. *Carbohydr Polym*. 2019;203:52-59. DOI: 10.1016/j.carbpol.2018.09.032.
10. Moradi S, Khani S, Ansari M, Shahlaei M. Atomistic details on the mechanism of organophosphates resistance in insects: insights from homology modeling, docking and molecular dynamic simulation. *J Mol Liq*. 2019;276:59-66. DOI: 10.1016/j.molliq.2018.11.152.
11. Wu D, Yan J, Wang J, Wang Q, Li H. Characterisation of interaction between food colourant allura red AC and human serum albumin: multispectroscopic analyses and docking simulations. *Food Chem*. 2015;170:423-429. DOI: 10.1016/j.foodchem.2014.08.088.
12. Zhao L, Guo R, Sun Q, Lan J, Li H. Interaction between azo dye Acid Red 14 and pepsin by multispectral methods and docking studies. *Luminescence*. 2017;32(7):1123-1130. DOI: 10.1002/bio.3298.
13. Moradi S, Farhadian N, Balaei F, Ansari M, Shahlaei M. Multi spectroscopy and molecular modeling aspects related to drug interaction of aspirin and warfarin with pepsin; structural change and protease activity. *Spectrochim Acta A Mol Biomol Spectrosc*. 2020;228:117813,1-29. DOI: 10.1016/j.saa.2019.117813.
14. Krejpcio Z, Wojciak R. The influence of Al³⁺ ions on pepsin and trypsin activity *in vitro*. *Pol J Environ Stud*. 2002;11(3):251-254.
15. Morris GM, Huey R, Olson AJ. Using autodock for ligand-receptor docking. *Curr Protoc Bioinformatics*. 2008;24(1):8.14.1-8.14.40. DOI: 10.1002/0471250953.bi0814s24.
16. Morshedi D, Kesejini TS, Aliakbari F, Karami-Osboo R, Shakibaei M, Marvian AT, *et al*. Identification and characterization of a compound from Cuminum cyminum essential oil with antifibrillation and cytotoxic effect. *Res Pharm Sci*. 2014;9(6):431-443.
17. Berman HM, Westbrook J, Feng Z, Gilliland G, Bhat TN, Weissig H, *et al*. The protein data bank. *Nucleic Acids Res*. 2000;28(1):235-242. DOI: 10.1093/nar/28.1.235.
18. Rose PW, Beran B, Bi C, Bluhm WF, Dimitropoulos D, Goodsell DS, *et al*. The RCSB protein data bank: redesigned web site and web services. *Nucleic Acids Res*. 2011;39(Database issue):D392-D401. DOI: 10.1093/nar/gkq1021.
19. Jalali F, Dorraji PS, Mahdiuni H. Binding of the neuroleptic drug, gabapentin, to bovine serum albumin: insights from experimental and computational studies. *J Lumin*. 2014;148:347-352. DOI: 10.1016/j.jlumin.2013.12.046.
20. Hanwell MD, Curtis DE, Lonie DC, Vandermeersch T, Zurek E, Hutchison GR. Avogadro: an advanced semantic chemical editor, visualization, and analysis platform. *J Cheminform*. 2012;4(1):17-33. DOI: 10.1186/1758-2946-4-17.
21. Bijari N, Moradi S, Ghobadi S, Shahlaei M. Elucidating the interaction of letrozole with human serum albumin by combination of spectroscopic and molecular modeling techniques. *Res Pharm Sci*. 2018;13(4):304-315. DOI: 10.4103/1735-5362.235157.
22. Malde AK, Zuo L, Breeze M, Stroet M, Poger D, Nair PC, *et al*. An automated force field topology builder (ATB) and repository: version 1.0. *J Chem Theory Comput*. 2011;7(12):4026-4037. DOI: 10.1021/ct200196m.
23. Van Der Spoel D, Lindahl E, Hess B, Groenhof G, Mark AE, Berendsen HJ. GROMACS: fast, flexible, and free. *J Comput Chem*. 2005;26(16):1701-1718. DOI: 10.1002/jcc.20291.
24. Banisharif-Dehkordi F, Mobini-Dehkordi M, Shakhshi-Niaei M, Mahnam K. Design and molecular dynamic simulation of a new double-epitope tolerogenic protein as a potential vaccine for multiple sclerosis disease. *Res Pharm Sci*. 2019;14(1):20-26. DOI: 10.4103/1735-5362.251849.
25. Wang K, Hu F, Xu K, Cheng H, Jiang M, Feng R, *et al*. CASCADE_SCAN: mining signal transduction network from high-throughput data based on steepest descent method. *BMC bioinformatics*. 2011;12(1):164-178. DOI: 10.1186/1471-2105-12-164.

26. Bussi G, Donadio D, Parrinello M. Canonical sampling through velocity rescaling. *J Chem Phys.* 2007;126(1):014101,1-8.
DOI: 10.1063/1.2408420.
27. Hess B, Kutzner C, Van Der Spoel D, Lindahl E. GROMACS 4: algorithms for highly efficient, load-balanced, and scalable molecular simulation. *J Chem Theory Comput.* 2008;4(3):435-447.
DOI: 10.1021/ct700301q.
28. Vaiwala R, Jadhav S, Thaokar R. Electrostatic interactions in dissipative particle dynamics Ewald-like formalism, error analysis, and pressure computation. *J Chem Phys.* 2017;146(12):124904, 1-10.
DOI: 10.1063/1.4978809.
29. Raza S, Azam SS. AFD: an application for bi-molecular interaction using axial frequency distribution. *J Mol Model.* 2018;24(4):84-92.
DOI: 10.1007/s00894-018-3601-3.
30. Mojaddami A, Sakhteman A, Fereidoonzehad M, Faghieh Z, Najdian A, Khabnadideh S, et al. Binding mode of triazole derivatives as aromatase inhibitors based on docking, protein ligand interaction fingerprinting, and molecular dynamics simulation studies. *Res Pharm Sci.* 2017;12(1):21-30.
DOI: 10.4103/1735-5362.199043.
31. Yan J, Zhang G, Hu Y, Ma Y. Effect of luteolin on xanthine oxidase: inhibition kinetics and interaction mechanism merging with docking simulation. *Food Chem.* 2013;141(4):3766-3773.
DOI: 10.1016/j.foodchem.2013.06.092.
32. Ghalandari B, Divsalar A, Saboury AA, Haertlé T, Parivar K, Bazl R, et al. Spectroscopic and theoretical investigation of oxali-palladium interactions with β -lactoglobulin. *Spectrochim Acta A Mol Biomol Spectrosc.* 2014;118:1038-1046.
DOI: 10.1016/j.saa.2013.09.126.
33. Ahmadi F, Ebrahimi-Dishabi N, Mansouri K, Salimi F. Molecular aspect on the interaction of zinc-ofloxacin complex with deoxyribonucleic acid, proposed model for binding and cytotoxicity evaluation. *Res Pharm Sci.* 2014;9(5):367-383.
34. Hou HN, Qi ZD, Ouyang YW, Liao FL, Zhang Y, Liu Y. Studies on interaction between Vitamin B12 and human serum albumin. *J Pharm Biomed Anal.* 2008;47(1):134-139.
DOI: 10.1016/j.jpba.2007.12.029.
35. Ranjbar S, Ghobadi S, Khodarahmi R, Nemati H. Spectroscopic characterization of furosemide binding to human carbonic anhydrase II. *Int J Biol Macromol.* 2012;50(4):910-917.
DOI: 10.1016/j.ijbiomac.2012.02.005.
36. Lakowicz JR, Malicka J, Gryczynski I, Gryczynski Z, Geddes CD. Radiative decay engineering: the role of photonic mode density in biotechnology. *J Phys D Appl Phys.* 2003;36(14):R240-R249.
DOI: 10.1088/0022-3727/36/14/203.
37. Wu X, Liu J, Wang Q, Xue W, Yao X, Zhang Y, et al. Spectroscopic and molecular modeling evidence of clozapine binding to human serum albumin at subdomain IIA. *Spectrochim Acta A Mol Biomol Spectrosc.* 2011;79(5):1202-1209.
DOI: 10.1016/j.saa.2011.04.043.
38. Chaturvedi SK, Ahmad E, Khan JM, Alam P, Ishtikhar M, Khan RH. Elucidating the interaction of limonene with bovine serum albumin: a multi-technique approach. *Mol Biosyst.* 2015;11(1):307-316.
DOI: 10.1039/c4mb00548a.
39. Balaei F, Ghobadi S. Hydrochlorothiazide binding to human serum albumin induces some compactness in the molecular structure of the protein: a multi-spectroscopic and computational study. *J Pharm Biomed Anal.* 2019;162:1-8.
DOI: 10.1016/j.jpba.2018.09.009.
40. Gao W, Li N, Chen Y, Xu Y, Lin Y, Yin Y, et al. Study of interaction between syringin and human serum albumin by multi-spectroscopic method and atomic force microscopy. *J Mol Struct.* 2010; 983(1-3):133-140.
DOI: 10.1016/j.molstruc.2010.08.042.
41. Moradi N, Ashrafi-Kooshk MR, Ghobadi S, Shahlaei M, Khodarahmi R. Spectroscopic study of drug-binding characteristics of unmodified and *p*NPA-based acetylated human serum albumin: does esterase activity affect microenvironment of drug binding sites on the protein? *J Lumin.* 2015;160:351-361.
DOI: 10.1016/j.jlumin.2014.11.019.
42. Xu ZQ, Yang QQ, Lan JY, Zhang JQ, Peng W, Jin JC, et al. Interactions between carbon nanodots with human serum albumin and γ -globulins: the effects on the transportation function. *J Hazard Mater.* 2016;301:242-249.
DOI: 10.1016/j.jhazmat.2015.08.062.
43. Naik PN, Nandibewoor ST, Chimatadar SA. Non-covalent binding analysis of sulfamethoxazole to human serum albumin: fluorescence spectroscopy, UV-vis, FT-IR, voltammetric and molecular modeling. *J Pharm Anal.* 2015;5(3):143-152.
DOI: 10.1016/j.jpha.2015.01.003.